

# Functional and structural conservation of CBS domains from CLC chloride channels

Raúl Estévez<sup>1</sup>, Michael Pusch<sup>2</sup>, Carles Ferrer-Costa<sup>3</sup>, Modesto Orozco<sup>3</sup> and Thomas J. Jentsch<sup>1</sup>

<sup>1</sup>Zentrum für Molekulare Neurobiologie Hamburg (ZMNH), Hamburg University, Falkenried 94, D-20246 Hamburg, Germany

<sup>2</sup>Istituto di Biofisica, Via de Marini 6, I-16149 Genova, Italy

<sup>3</sup>Departament de Bioquímica i Biologia Molecular, Facultat de Química, Universitat de Barcelona, Martí i Franques 1, Barcelona 08028, and Institut de Recerca Biomèdica, Parc Científic de Barcelona, Josep Samitier 1–5, Barcelona 08028, Spain

**All eukaryotic CLC Cl<sup>-</sup> channel subunits possess a long cytoplasmic carboxy-terminus that contains two so-called CBS (cystathionine β-synthase) domains. These domains are found in various unrelated proteins from all phylae. The crystal structure of the CBS domains of inosine monophosphate dehydrogenase (IMPDH) is known, but it is not known whether this structure is conserved in CLC channels. Working primarily with CLC-1, we used deletion scanning mutagenesis, coimmunoprecipitation and electrophysiology to demonstrate that its CBS domains interact. The replacement of CBS domains of CLC-1 with the corresponding CBS domains from other CLC channels and even human IMPDH yielded functional channels, indicating a high degree of structural conservation. Based on a homology model of the pair of CBS domains of CLC channels, we identified some residues that, when mutated, affected the common gate which acts on both pores of the dimeric channel. Thus, we propose that the structure of CBS domains from CLC channels is highly conserved and that they play a functional role in the common gate.**

(Received 20 November 2003; accepted after revision 5 January 2004; first published online 14 January 2004)

**Corresponding author** T. J. Jentsch: Zentrum für Molekulare Neurobiologie Hamburg (ZMNH), Hamburg University, Falkenried 94, D-20246 Hamburg, Germany. Email: jentsch@zmnh.uni-hamburg.de

Chloride channels from the CLC family are important for several physiological functions such as the excitability of skeletal muscle (Steinmeyer *et al.* 1991), the transport of salt and water in the kidney (Simon *et al.* 1997; Matsumura *et al.* 1999; Estévez *et al.* 2001), and the acidification of intracellular vesicles in the endosomal–lysosomal pathway (Piwon *et al.* 2000; Kornak *et al.* 2001; Stobrawa *et al.* 2001). Several human genetic diseases are caused by mutations in members of this family (Koch *et al.* 1992; Lloyd *et al.* 1996; Simon *et al.* 1997; Birkenhäger *et al.* 2001; Kornak *et al.* 2001).

At the single-channel level, the activity of the Cl<sup>-</sup> channel CLC-0 from *Torpedo* shows three equally spaced current levels that appear in bursts (Miller & White, 1984; Bauer *et al.* 1991; Middleton *et al.* 1994). It was proposed that the channel possesses a ‘double-barrelled’ mode of gating: a fast gate acting on single protopores and a common slow gate that closes both pores simultaneously. This model was strongly supported by mutagenesis data (Ludewig *et al.* 1996; Middleton *et al.* 1996; Weinreich &

Jentsch, 2001) that provided evidence for a homodimer with one pore per subunit. In full agreement with these hypotheses, the recent crystal structure from two bacterial CLC channels showed homodimers in which each subunit forms a pore (Dutzler *et al.* 2002). The structure of bacterial CLC proteins is conserved with high fidelity in their mammalian counterparts (Estévez *et al.* 2003). Whereas the double-pore structure almost certainly holds true for all CLC channels, the assignment ‘fast’ to the individual gate and ‘slow’ to the common gate applies for the *Torpedo* channel CLC-0, but not for CLC-1, for example (Saviane *et al.* 1999).

The gating of some CLC channels depends strongly on the permeating anion (Richard & Miller, 1990; Pusch *et al.* 1995a). It has been proposed that a Cl<sup>-</sup> anion must reach a binding site in the pore in order to open the channel (Pusch *et al.* 1995a; Chen & Miller, 1996). The crystal structure of bacterial CLC proteins revealed that the side chain of a highly conserved glutamate protrudes into the pore. It was suggested that it might represent an important structural

component of the Cl<sup>-</sup>-dependent 'fast' gate that closes the pores of the double-pore channel individually (Dutzler *et al.* 2002, 2003).

The common gate in CLC channels is also Cl<sup>-</sup>-dependent (Chen & Miller, 1996; Pusch *et al.* 1999). Its gating transitions may require rather large conformational changes as inferred from its strong temperature dependence (Pusch *et al.* 1997). Some insights into structures influencing this gating process came from mutations in dominant myotonia (which affect the common gate) (Saviane *et al.* 1999). Several mutations were found in helices that were either involved in subunit-subunit interactions or were close to the anion-binding site (Estévez & Jentsch, 2002). Moreover, mutagenesis studies revealed the importance of carboxy-terminal cytoplasmic structures and of the last helix R, that connects these structures to the transmembrane part. Thus, some mutations in the R-helix affected slow gating (Ludewig *et al.* 1997), and several chimeras in which carboxy-terminal segments were exchanged between ClC-0, -1 and -2 had drastically changed 'slow' gating (Fong *et al.* 1998).

All eukaryotic CLC proteins have a long carboxy-terminal cytoplasmic region that contains two copies of a 'CBS domain' (from cystathionine- $\beta$ -synthase). These structural domains normally occur in pairs and are found in several, otherwise diverse, proteins from all organisms. They have three  $\beta$ -strands and two  $\alpha$ -helices (Bateman, 1997; Ponting, 1997). The CBS domains from the enzyme IMPDH have been crystallized (Sintchak *et al.* 1996; Zhang *et al.* 1999). Their crystal structure revealed that the two CBS domains of this protein contacted each other within the same protein, and that their interaction was mainly mediated by  $\beta$ -strands. The two  $\alpha$ -helices of CBS domains are amphipathic. Their hydrophobic amino acids point to the interior and charged amino acids are located at the surface.

Several functions have been proposed for CBS domains. It has been suggested that they play a role in the oligomerization (Jhee *et al.* 2000) and regulation (Shan *et al.* 2001) of cystathionine  $\beta$ -synthase. Alanine-scanning mutagenesis of the yeast Cl<sup>-</sup> channel ScClC (gef1p) suggested that CBS domains influenced the subcellular localization of the channel (Schwappach *et al.* 1998). However, it is safe to state that the function of CBS domains is still very poorly understood. The biological importance of these domains, on the other hand, is underscored by point mutations in CBS domains of several unrelated proteins that result in various human inheritable diseases (Koch *et al.* 1992; Lloyd *et al.* 1996; Simon *et al.* 1997; Shan & Kruger, 1998; Milan *et al.* 2000; Blair *et al.* 2001; Cleiren

*et al.* 2001; Kornak *et al.* 2001; Bowne *et al.* 2002; Kennan *et al.* 2002).

When ClC-0 or ClC-1 Cl<sup>-</sup> channels were truncated after the first CBS domain, they did not give rise to currents (Schmidt-Rose & Jentsch, 1997; Maduke *et al.* 1998). Their function could be restored by co-expressing the missing carboxy-terminal part containing the second CBS domain. In the present study, we used several approaches to show that the CBS domains located on the amino- and carboxy-terminal parts of these split channels interact and are largely interchangeable. Exchanges of CBS domains as well as specific point mutations affecting residues at their surfaces changed voltage-dependent gating through the common gate that affects both pores.

## Methods

### Functional expression in *Xenopus* oocytes

Capped complementary RNA of CLC channels (ClC-1: 10 ng, ClC-0: 1 ng) was expressed in *Xenopus* oocytes as previously described (Estévez *et al.* 2001). Measurements were made in ND96 medium (96 mM NaCl, 2 mM KCl, 1.8 mM CaCl<sub>2</sub>, 1 mM MgCl<sub>2</sub> and 5 mM Hepes buffer at pH 7.4). Pulse protocols for tail current analysis of ClC-1 were performed as described in Pusch *et al.* (1995a). Briefly, after stepping the voltage from +100 to -140 mV in 20 mV steps for 500 ms, channel activation was monitored at -80 mV. Extrapolated peak currents were fitted using a Boltzmann distribution of the form  $I(V) = I_0 + I_{\max}/(1 + \exp(zF(V_{0.5} - V)/RT))$ , where  $I_{\max}$  is the extrapolated current at maximal stimulation,  $z$  is the apparent gating charge,  $V_{0.5}$  is the voltage of half-maximal activation,  $I_0$  is a constant offset describing the minimal open probability,  $P_{o,\min}$ ,  $V$  is the voltage,  $R$  is the gas constant and  $T$  is the absolute temperature. Fast and slow gates of ClC-0 were studied using protocols previously described (Ludewig *et al.* 1997; Pusch *et al.* 2001). To study the fast gate, the slow gate was opened by hyperpolarizing prepulses. It is sufficiently slow to remain open during the subsequent pulse protocol used to study fast gating. Fast gates were maximally opened by a short prepulse to +60 mV, followed by steps to test voltages between +60 and -140 mV. The open probability of the fast gate was determined by subsequently stepping to -100 mV and extrapolating currents to the beginning of the pulse. It was normalized to the maximum current to yield the apparent  $P_{o,\text{fast}} \cdot P_{o,\text{fast}} = f(V)$  was fitted with a Boltzmann distribution containing a variable offset  $P_{\min}$ , similar to that described for ClC-1 activation gating. Steady-state activation of the slow, common gate was studied by stepping the voltage

for 6 s each to values from +60 to -140 mV in steps of 20 mV. Channel activation was monitored directly after each pulse at a constant potential of +40 mV. A single Boltzmann distribution with a variable offset was sufficient to describe the steady state of slow gating. The Clampfit program (Axon Instruments) was used for fitting. Two batches of oocytes were used, with each batch containing  $n = 6$  oocytes.

### Determination of inhibition by extracellular $Zn^{2+}$

Oocytes were superfused with the standard extracellular solution (ND96) that contained in addition 10 or 100  $\mu M$   $ZnCl_2$ . The onset of inhibition was monitored by the repetitive application of pulses to +60 mV (50 ms duration) and -140 mV (200 ms duration) every 12 s until a steady state was reached. Figure 6B reports the ratio between the current measured at +60 mV after reaching steady state and the current before the application of  $Zn^{2+}$ .

### Patch clamp analysis

Inside-out patch clamp experiments were performed using an EPC-7 amplifier (List, Darmstadt, Germany) and the Pulse program (HEKA, Lambrecht, Germany). The standard intracellular solution contained (mM) 100 NMDG-Cl, 2  $MgCl_2$ , 10 HEPES, 2 EGTA at pH 7.3; the standard extracellular solution contained 100 NMDG-Cl, 5  $MgCl_2$ , 10 HEPES.

### Molecular biology

Constructs were made using recombinant PCR and sequenced. In ClC-1, a haemagglutinin (HA) epitope was introduced between helices L and M after the glycosylation site, resulting in the sequence 'VKHAG **YPYDVDPDYADPES**' (HA epitope in bold). In the N-terminus of ClC-1 and  $N_{1-720}$ , a HA or a myc epitope ('**MEEQKLISEEDLQS**') was added after the second amino acid. These tags did not significantly affect conductances or the voltage dependence of gating.

### Oocyte membrane isolation, coimmunoprecipitations, and Western blot analysis

Oocytes were homogenized in an ice-cold solution (buffer A) containing 150 mM NaCl, 5 mM Tris-HCl (pH 7.4), 1% Triton X-100 and a protease inhibitor mix (Complete, Roche). Yolk platelets were removed by three low speed centrifugations. For immunoprecipitation, the antibody (HA: 3F10, Roche; myc: 9E10, ATCC hybridoma) was

added to the supernatant. After an incubation at 4°C for 2 h, the solution was mixed with protein G coupled to agarose beads pre-equilibrated in buffer A and incubated a further 3 h. The pellet obtained by centrifugation was then washed 5 times with buffer A and mixed with SDS-Laemmli sample buffer containing 50 mM DTT and heated for 15 min at 55°C to elute it from the beads. Western blot analysis was performed as previously described (Schwake *et al.* 2000).

### Measurement of surface expression

Surface expression using HA antibodies and chemiluminescence was performed as previously described (Zerangue *et al.* 1999; Schwake *et al.* 2000). Briefly, oocytes were placed for 30 min in ND96 with 1% bovine serum albumin (BSA) at 4°C, then incubated for 60 min at 4°C with 1  $\mu g ml^{-1}$  rat monoclonal anti-HA antibody (3F10, Roche) in 1% BSA-ND96, washed at 4°C, and incubated with horseradish peroxidase-coupled secondary antibody (goat anti-rat Fab fragments, Jackson ImmunoResearch, in 1% BSA for 30–60 min at 4°C). Oocytes were washed thoroughly (1% BSA, 4°C, 60 min) and transferred to ND96 without BSA. Individual oocytes were placed in 50  $\mu l$  of Power Signal Elisa solution (Pierce). Chemiluminescence was quantified in a Turner TD-20/20 luminometer (Turner BioSystems, Sunnyvale, CA, USA). Data shown were obtained with  $n = 10$  oocytes.

### Molecular modelling

The X-ray structure of the CBS domains of IMPDH from *Streptococcus pyogenes* (protein database code 1zjf) was used as template to model the CBS domains of ClC-1. The alignment of multiple CBS domains in the corresponding Pfam family (Pfam family PF00571, see Bateman (1997)) was used to determine the boundaries of the CBS domains of ClC-1 and to obtain a first alignment of these domains to those present in IMPDH. This preliminary alignment was then refined using the ALIGN-2D procedure of the MODELLER program (Sali & Blundell, 1993). Such a procedure maintains the general alignment reported in the corresponding Pfam family or on the SMART web page, but optimizes the location of the gaps to build a reliable 3-D model. The quality of the resulting alignments was verified by comparison with Pfam families, as well as with the control tools in MODELLER (Sali & Blundell, 1993). The final alignments show 16% (CBS1) and 21% (CBS2) identity with the CBS domains of IMPDH from *Streptococcus pyogenes*.

Once the two CBS domains of CIC-1 were independently aligned, a chimera consisting of the two CBS domains of CIC-1 plus the connecting segment between both domains of IMPDH was generated *in silico*. This final aligned sequence was then used to build a model using the standard procedure in MODELLER (Sali & Blundell, 1993). Five models were generated and checked for potential energy and stereochemistry. In all cases the suggested models were similar and showed good energetic and stereochemical properties. Finally, the five models were checked against the template using PROSAIL (Sippl, 1993). The energy profiles and *Z*-score for all the models were close to the pdb template. The lowest energy model was selected.

## Results

### The C-terminal region in CIC-1 is not needed for dimerization

It was shown that a non-functional mutant of CIC-1 that is truncated after residue 720 ( $N_{1-720}$ ) could be complemented by co-expressing the missing C-terminal part ( $C_{721-988}$ ) from a separate construct (Schmidt-Rose & Jentsch, 1997; Fig. 1A). Similar results were obtained with CIC-0 (Maduke *et al.* 1998). These truncations occurred in the cytoplasmic tail between the two CBS domains. To determine whether  $N_{1-720}$  needs  $C_{721-988}$  for its transport

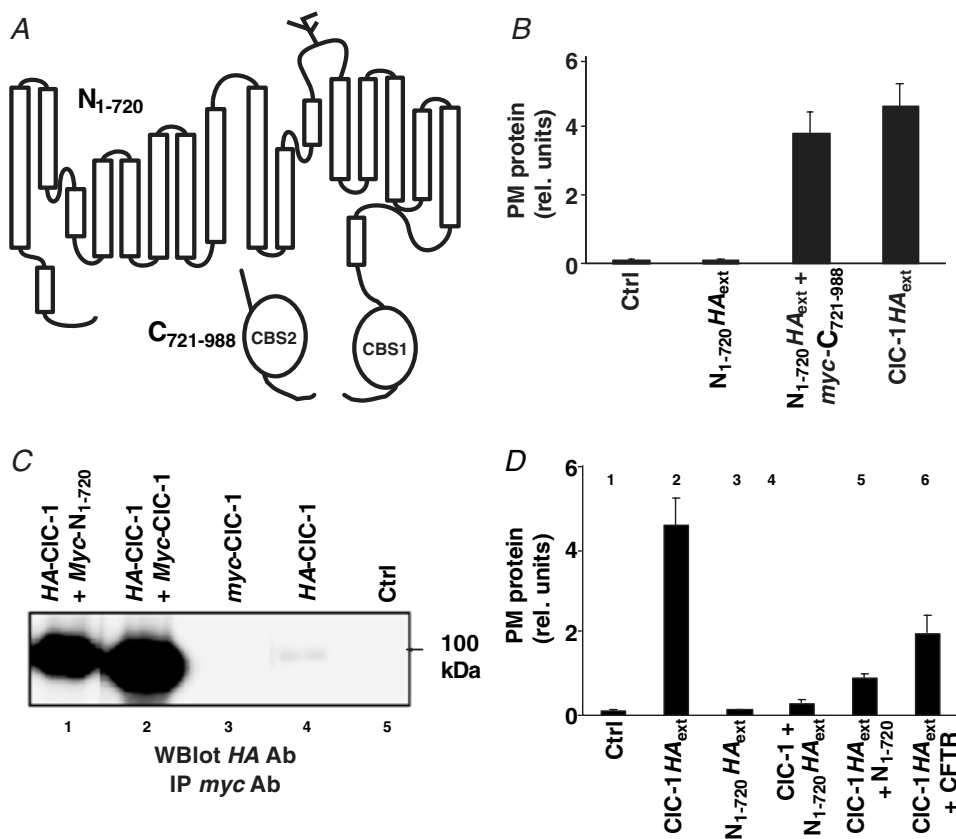


**Figure 1. Biochemical and functional analysis of complementation between  $N_{1-720}$  and  $C_{721-988}$**

**A**, schematic representation of the CIC-1 channel split between the two CBS domains. **B**, plasma membrane (PM) levels of  $N_{1-720}$  and CIC-1 tagged with extracellular HA epitopes. Surface expression, as determined by a chemiluminescence assay (Zerangue *et al.* 1999; Schwake *et al.* 2000), is given in relative units.  $N_{1-720}$  reaches the surface only upon co-expression with  $C_{721-988}$  (tagged with a myc epitope). Averages of  $\geq 10$  oocytes are shown. Another experiment gave similar results. **C**, coimmunoprecipitation using epitope-tagged versions of CIC-1 and  $N_{1-720}$  expressed in oocytes. Solubilized membrane proteins were precipitated with the HA antibody and detected in Western blotting by the myc antibody. A second independent experiment gave similar results. **D**, effect of co-expressing CIC-1 and  $N_{1-720}$  on surface expression in oocytes. Surface-expressed CIC-1 and  $N_{1-720}$  tagged with extracellular HA epitopes were detected using a chemiluminescence assay as in **B**.

to the surface, which could explain the failure of  $N_{1-720}$  to yield currents, we inserted an *HA* tag in the extracellular loop between helices L and M of  $N_{1-720}$ . Tagged  $N_{1-720}$  was then expressed in *Xenopus* oocytes, either alone or together with a *myc*-tagged version of  $C_{721-988}$ . Monitoring the surface expression of  $HA-N_{1-720}$  with an *HA* antibody revealed that  $N_{1-720}$  does not reach the plasma membrane by itself (Fig. 1B). When co-expressed with  $C_{721-988}$ , however, surface expression was similar to that of full-length *CIC-1*.

To test whether  $N_{1-720}$  is able to physically interact with wild-type *CIC-1*, coimmunoprecipitation experiments (Fig. 1C) and surface expression assays (Fig. 1D) were performed in the oocyte expression system.

As shown in Fig. 1C, *HA-CIC-1* came down with *myc-N<sub>1-720</sub>* (lane 1) to a similar extent as with *myc-CIC-1* (lane 2) when extracts of oocytes co-expressing these constructs were precipitated with *HA* antibodies. Only very faint bands were observed in uninjected oocytes or in oocytes injected only with *myc-CIC-1* or *HA-CIC-1*, confirming the specificity of these results.

In the second set of experiments, we checked whether the co-expression of  $N_{1-720}$  influenced the surface expression of *CIC-1* and vice versa, using *HA*-tagged proteins in the oocyte system. As described above, *CIC-1*, but not  $N_{1-720}$ , reached the surface of oocytes (Fig. 1D, lanes 2 and 3). Co-expressing  $N_{1-720}$  with *CIC-1* did not lead to a substantial increase in the surface expression of tagged  $N_{1-720}$

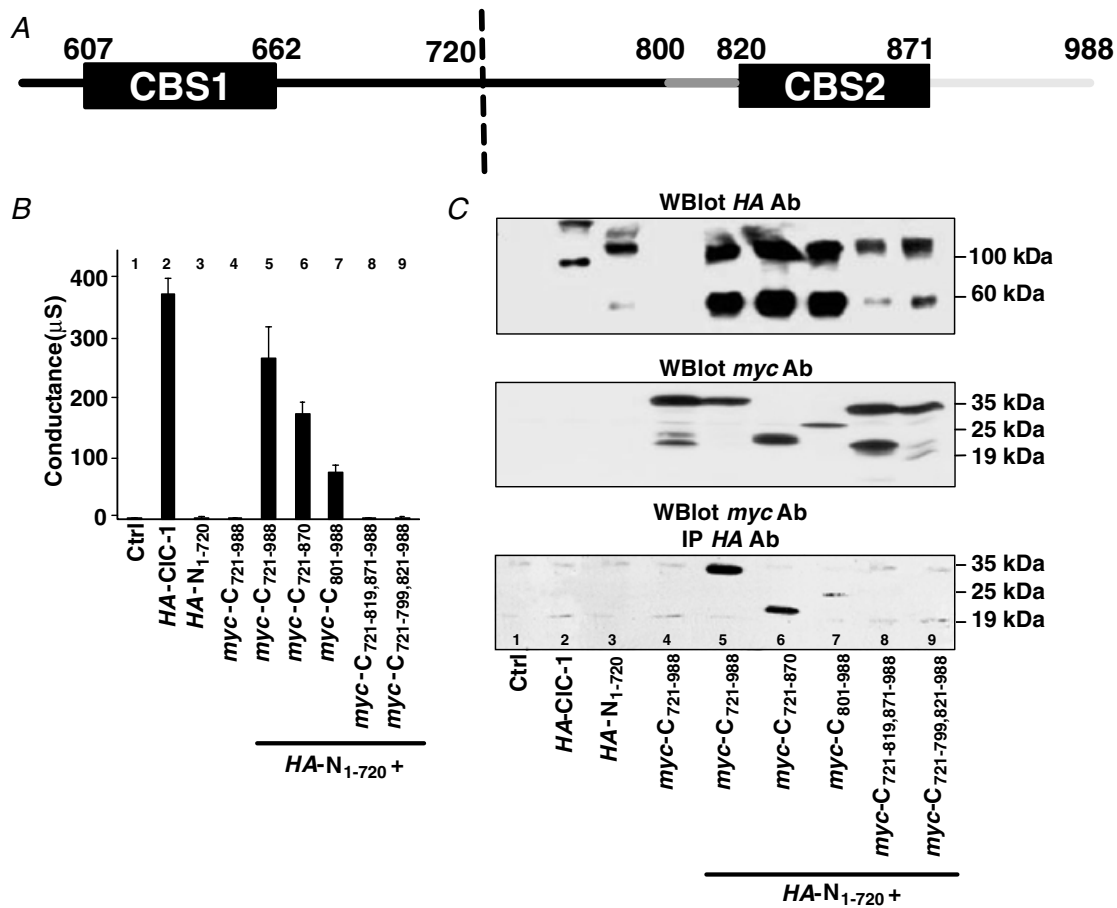


**Figure 2. Regions needed for the functional complementation between  $N_{1-720}$  and  $C_{721-988}$**

A, schematic representation of the carboxy-terminal region of *CIC-1* that was analysed by mutagenesis. B, conductance levels (at 0 mV, in  $\mu$ S) of key constructs after expression in *Xenopus* oocytes. C, biochemical analysis of proteins analysed electrophysiologically in A and indicated below the different lanes. Western blot analysis of oocyte membranes for *HA-N<sub>1-720</sub>* using the 3F10 antibody against *HA* epitope (top panel), and for *myc-C<sub>721-988</sub>* constructs using the 9E10 antibody against the *myc* epitope (centre panel). Lower panel, immunoprecipitation of solubilized oocyte membranes using the *HA* antibody for precipitation and the *myc* antibody for detection in Western blotting. Three independent experiments gave similar results.

**Table 1. Comparative summary of currents and voltage dependence of gating**

	$V_{0.5}$ (mV)
<b>Controls</b>	
CIC-1	$-68.5 \pm 1.2$
$N_{1-720} + C_{721-988}$	$-70.4 \pm 4.5$
$N_{1-720} + C$ - and $N$ - deletions of $C_{721-988}$	
$C_{721-870} + N_{1-720}$	$-20.4 \pm 6.4$
$C_{721-858} + N_{1-720}$	n.c.
$C_{721-826} + N_{1-720}$	n.c.
$C_{801-988} + N_{1-720}$	$-65.7 \pm 1.8$
$C_{821-988} + N_{1-720}$	n.c.
<b>C-deletions of <math>N_{1-720}</math></b>	
$N_{1-679} + C_{721-988}$	$-80.7 \pm 2.7$
$N_{1-679} + C_{821-988}$	$-58.7 \pm 2.0$
$N_{1-665} + C_{721-988}$	n.c.
$N_{1-653} + C_{721-988}$	n.c.
<b>Internal deletions of <math>C_{721-988}</math> and <math>N_{1-720}</math></b>	
$C_{721-819,872-988} + N_{1-720}$	n.c.
$C_{721-819,841-988} + N_{1-720}$	n.c.
$C_{721-840,872-988} + N_{1-720}$	n.c.
$C_{721-799,821-988} + N_{1-720}$	n.c.
$C_{721-799,807-988} + N_{1-720}$	$-59.8 \pm 1.8$
$C_{721-806,814-988} + N_{1-720}$	n.c.
$C_{721-813,821-988} + N_{1-720}$	$-51.2 \pm 0.8$
$N_{1-606,627-720} + C_{721-988}$	n.c.
$N_{1-626,661-720} + C_{721-988}$	n.c.
<b>Deletions in CIC-1</b>	
CIC-1del(820-871)	$-31.7 \pm 2.7$
CIC-1del(800-820)	n.c.
CIC-1del(666-780)	$-61.8 \pm 2.2$
CIC-1del(627-660)	n.c.

The value of  $V_{0.5}$  (in mV) for wild-type CIC-1, truncation constructs, and co-expressed mutants was calculated as described in Methods. Results are from  $n = 4$  oocytes. n.c. indicates that no currents due to CIC-1 could be detected.

(lane 4), but  $N_{1-720}$  reduced the surface expression of tagged CIC-1 (lane 5). To test whether the latter reduction in surface expression might be explained by non-specific competition for translation or transport, we co-expressed CIC-1 with cystic fibrosis transmembrane conductance regulator (CFTR) in equimolar amounts (lane 6). Co-expression with CFTR reduced the surface expression of the tagged CIC-1 protein by a factor of two. This suggested that the  $\sim 50\%$  decrease is due to a saturation of the translation/trafficking machinery. By contrast, the  $> 75\%$  reduction in surface expression of CIC-1 caused by  $N_{1-720}$  (lane 5) suggested a specific interaction that led to an intracellular retention of CIC-1- $N_{1-720}$  dimers. Such retention may also explain the failure of CIC-1 to increase the surface expression of  $N_{1-720}$  (Fig. 1D, lane 4).

### Mapping regions needed for carboxy-terminal interactions

The experiments described above suggest that  $N_{1-720}$  could dimerize, but was unable to reach the plasma membrane. The missing C-terminal fragment that contains CBS2 was able to functionally rescue  $N_{1-720}$  only when expressed as a fragment ( $C_{721-988}$ ), but not when present in the wild-type (WT) CIC-1 protein.

We therefore investigated which parts of the CIC-1 carboxy-terminus (Fig. 2A) are needed for this functional rescue. We performed a systematic deletion scanning mutagenesis from the C- and N-terminus of  $C_{721-988}$  and constructed C-terminal deletions of  $N_{1-720}$ . We then created some internal deletions in  $C_{721-988}$ ,  $N_{1-720}$  and CIC-1 (see Table 1 for a list of constructs). These constructs were co-expressed in oocytes either with  $N_{1-720}$  (further deletions in the C-terminal fragment) or with  $C_{721-988}$  (N-terminal fragments) and their currents determined by two-electrode voltage clamping. When possible, the voltage dependence of currents was determined, but many of these constructs did not yield measurable currents (Table 1). Several key mutants were analysed both by electrophysiology (Fig. 2B) and by Western blotting and immunoprecipitation (Fig. 2C).

We first focused on the region between CBS1 and CBS2. In CIC-1, the CBS1 domain ranges from amino acids 607 to 662 and CBS2 from residues 820 to 871. When the N-terminus of the C-terminal fragment was further truncated in construct  $C_{801-988}$ , which leaves only about 20 residues in front of CBS2 (Fig. 2A), co-expression with  $N_{1-720}$  still gave typical, albeit reduced, currents (Fig. 2B, lane 7). Western analysis showed that this truncated construct increased the abundance of co-expressed HA-tagged  $N_{1-720}$  (Fig. 2C, top panel, lane 7; compare to lane 3) to a similar extent as did  $C_{721-988}$  (lane 5), even though it was expressed to lower levels (Fig. 2C, centre panel). Similar to  $C_{721-988}$ ,  $myc$ - $C_{801-988}$  increased the amount of the putative  $\sim 55$  kDa monomer band of  $N_{1-720}$  in comparison to the  $\sim 100$  kDa band which probably represents an SDS-resistant dimer (Fig. 2C, top panel; compare lanes 2 and 7).  $myc$ - $C_{801-988}$  could be coprecipitated with HA- $N_{1-720}$  (Fig. 2C, bottom panel). The relevant  $\sim 25$  kDa band is faint, but must be compared to the corresponding input that also shows low abundance (centre panel).

Co-expressing  $C_{721-988}$  with the more severely truncated  $N_{1-679}$ , that truncated CIC-1 shortly after CBS1, also gave functional channels with only slightly changed voltage dependence. This was even true when  $N_{1-679}$  was co-expressed with  $C_{801-988}$  (Table 1). This indicated that

most of the region between the two CBS domains is not necessary for the interaction between  $N_{1-720}$  and  $C_{721-988}$  that allows surface expression and rescues channel function. In line with these results, an in-frame deletion in CIC-1 that removed residues 666–780 gave currents with reduced amplitude, but unchanged voltage dependence (Table 1).

However, when the 20 residues immediately preceding CBS2 were deleted in the construct  $C_{721-799,821-988}$ , co-expression with  $N_{1-720}$  did not give rise to measurable currents (Fig. 2B, lane 9).  $C_{721-799,821-988}$  also failed to increase the abundance of (i.e. 'stabilize')  $N_{1-720}$  (Fig. 2C, top panel, lane 9), and no coimmunoprecipitation with  $N_{1-720}$  was detectable (Fig. 2C, bottom panel). To narrow down the functionally important region within this stretch, we introduced three smaller deletions (800–806, 807–813 and 814–820) into  $C_{721-988}$  (see Table 1). Their analysis revealed that only the region of amino acids 807–813 was essential (Table 1).

Truncating  $C_{721-988}$  shortly after CBS2 in construct  $C_{721-870}$  gave a protein that yielded functional channels when co-expressed with  $N_{1-720}$  (Fig. 2B, lane 6) and that was able to interact with  $N_{1-720}$  (Fig. 2C lane 6, bottom panel) and to stabilize it (Fig. 2C, top panel). Unlike split channels in which stretches between CBS had been deleted, however, the truncation after CBS2 dramatically changed the voltage dependence of currents (Table 1).

In contrast, C-terminal fragments with deletions in CBS2 (820–871, 820–840, 841–871) did not give currents when co-expressed with  $N_{1-720}$  (see Table 1).  $C_{721-819,871-988}$ , in which CBS2 was completely absent, was not able to stabilize  $N_{1-720}$  (Fig. 2C lane 8, top panel

and could not be coimmunoprecipitated with  $HA-N_{1-720}$  (Fig. 2C, bottom panel). Likewise, co-expressing  $C_{721-988}$  with mutants of  $N_{1-720}$  that carry deletions in CBS1 (607–626 and 627–660) did not yield measurable currents (Table 1). Thus, both CBS domains are needed for plasma membrane expression and for the physical interaction of  $C_{721-988}$  with  $N_{1-720}$ . The easiest explanation is that CBS1 interacts with CBS2 and that this interaction enables  $N_{1-720}$  to reach the plasma membrane.

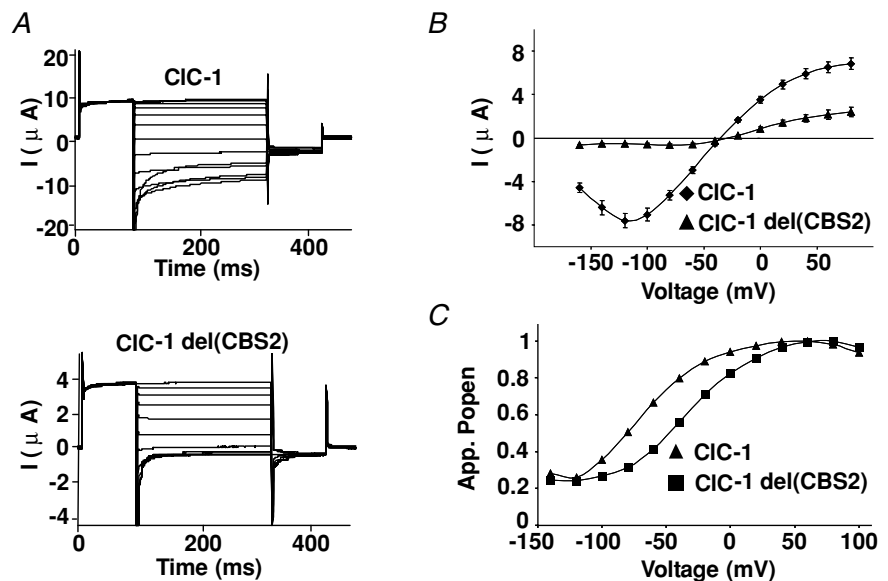
Western blot analysis indicated that not only is  $N_{1-720}$  stabilized by  $C_{721-988}$ , but that also the reverse is true (Fig. 2C, middle panel).  $C_{721-988}$  expressed by itself (lane 4) yielded a major band of  $\sim 35$  kDa and other bands of lower molecular weights (between  $\sim 19$  and  $\sim 25$  kDa). These bands probably corresponded to degradation products of  $C_{721-988}$ . In contrast, when  $C_{721-988}$  was co-expressed with  $N_{1-720}$ , only a  $\sim 35$  kDa band and a very weak band of  $\sim 25$  kDa were detectable (lane 5). This result suggested that  $C_{721-988}$  is stabilized by interacting with  $N_{1-720}$ . Similarly, no putative degradation products were detected with interaction-competent deletions of the C-terminal part, where co-expressed with  $N_{1-720}$  ( $C_{721-870}$  and  $C_{801-988}$ , lanes 6 and 7). However, such products were seen with constructs that probably failed to interact ( $C_{721-799,821-988}$  and  $C_{721-819,871-988}$ ) (Fig. 2C, middle panel, lanes 8 and 9).

### Deletion of the CBS2 domain affects gating in CIC-1

At first sight, the results showing that CBS2 is necessary for the formation of functional split channels (Table 1)

### Figure 3. Functional effects of deleting CBS2 in CIC-1

A, typical traces from two-electrode voltage clamp analysis of *Xenopus* oocytes expressing WT CIC-1 (upper panel), or a mutant in which CBS2 was totally deleted (lower panel). The oocytes were clamped between +100 and  $-140$  mV as described in Methods. B, current-voltage ( $I$ - $V$ ) curves averaged from 6 oocytes of one batch. Three independent experiments gave very similar results. C, tail current analysis from a representative oocyte. The voltage of half-maximal activation was  $-31.7 \pm 2.7$  mV ( $n = 10$ ) and  $-68.5 \pm 1.2$  mV ( $n = 68$ ) for CIC-1del(CBS2) and the wild-type channel, respectively, without a change in the slope of apparent  $P_{open}$  as a function of voltage.



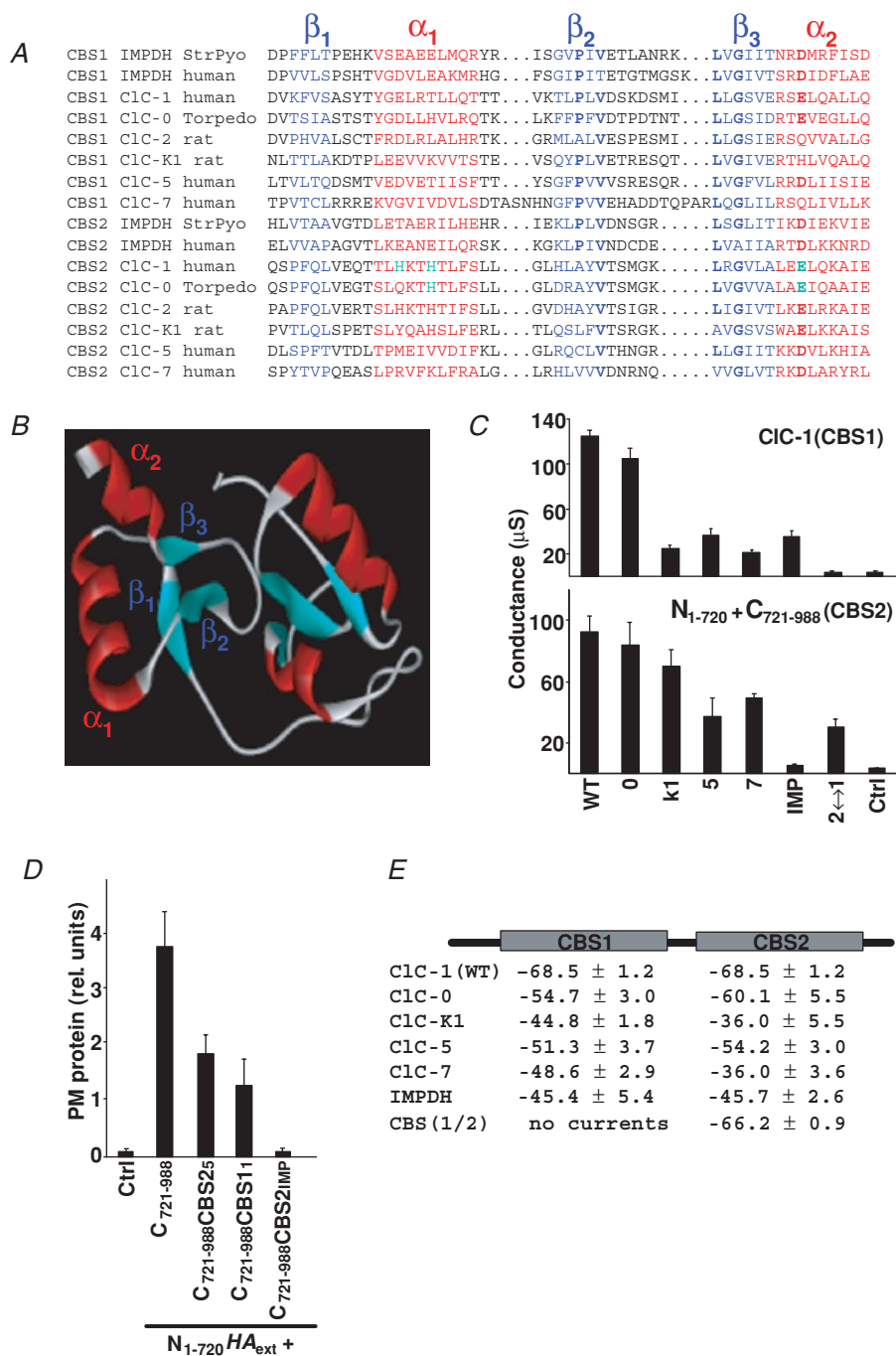


**Figure 4. Functional conservation of CBS domains**

A, alignment of CBS domains (CBS1, CBS2) from the various CLC channels used in this study with those from human and bacterial IMPDH. The 3-D structure of the dimer of CBS domains of the bacteria *S. pyogenes* (StrPyo) has been solved by crystallography (Zhang *et al.* 1999). A more extensive alignment of CBS domains from different proteins is available on the internet (<http://smart.embl-heidelberg.de>). Structural elements are highlighted by colours ( $\beta$ -strands in blue,  $\alpha$ -helices in red), while bold characters indicate some of the residues that are conserved between CBS domains. Green indicates amino acids that drastically changed gating when mutated. have been studied by mutagenesis. B, homology model of the dimer of CBS domains from CIC-1. For modelling purposes, the region between CBS domains was replaced by that of *S. pyogenes* IMPDH. C, conductances (at 0 mV, in  $\mu$ S) of CIC-1 chimeras in which either the CBS1 domain was exchanged in the otherwise intact channel protein (upper panel), or in which CBS2 was exchanged in C<sub>721-988</sub> to analyse split channels (lower panel). The proteins from which these CBS domains were taken are indicated below (0, C1C-0; K1, C1C-K1, etc.; IMP, human inosine monophosphate

seemed to contradict an earlier report (Hryciw *et al.* 1998) that described typical Cl<sup>-</sup> currents with an in-frame deletion within CBS2 of ClC-1 (deletion of amino acids 841–870, corresponding to D13 in the old nomenclature; Jentsch *et al.* 1999). Extending the observation of Hryciw *et al.* (1998), we found that even the complete deletion of CBS2 in ClC-1 (ClC-1del(820–871)) gave functional Cl<sup>-</sup> channels that had reduced current amplitudes (Fig. 3B) and a changed gating behaviour (Fig. 3C). The voltage of half-maximal activation was  $-31.7 \pm 2.7$  mV ( $n = 10$ ) for ClC-1del(820–871) ( $V_{0.5}(\text{WT}) = -68.5 \pm 1.2$  mV ( $n = 68$ )), without any change in the slope of  $P_{\text{open}}$  as a function of voltage (Fig. 3A and C).

This revealed that CBS2 *per se* is not essential for channel function in ClC-1, but may be needed to bring essential C-terminal domains into the proximity of the channel backbone of the split channel (possibly by binding to CBS1). Interestingly, in this respect similar to N<sub>1–720</sub> (Fig. 2C, top panel), ClC-1del(820–871) was predominantly detected as an SDS-resistant dimer in Western blot analysis (data not shown). Unlike the situation with CBS2 deletions, no currents were detected when CBS1 was deleted in ClC-1 (ClC-1del(627–660) (Table 1).

### CBS domains can be exchanged without abolishing channel function

The results obtained with various split channels are compatible with the notion that the CBS domains of CLC channels may interact. This would be analogous to the bacterial enzyme IMPDH, the crystal structure of which demonstrated an interaction of its CBS domains (Zhang *et al.* 1999). An alignment of CBS domains from various CLC channels and from human and bacterial IMPDH is shown in Fig. 4A. Although the degree of primary sequence homology between different CBS domains is low (15–40%), the conservation of some amino acids, in particular in the second and third  $\beta$ -strand, is obvious (in bold in Fig. 4A). Structural features like the amphipathic character of their  $\alpha$ -helices are very well conserved.

In view of this structural conservation, we asked whether the replacement of ClC-1 CBS domains by other CBS domains would be compatible with Cl<sup>-</sup> channel function. In the first set of experiments, CBS1 of ClC-1 was replaced by the corresponding CBS1 domains of several other CLC channels (ClC-0, -K1, -5 and -7), or by CBS1 of human IMPDH. Additionally, we replaced CBS1 by CBS2. With the exception of the latter construct, which duplicated CBS2 in the carboxy-terminus of ClC-1, all these constructs gave detectable currents after expression in oocytes. However, their amplitudes were mostly reduced (Fig. 4C, upper panel). In a second set of experiments, we replaced CBS2 in C<sub>721–988</sub> by the corresponding CBS2 domains from the same set of proteins as above, or by CBS1 from ClC-1. This ‘split channel’ approach also addresses the question of whether the new CBS domain allowed an interaction of the carboxy-terminal fragment containing changed CBS domains with the truncated channel protein. Electrophysiological analysis (Fig. 4C, lower panel) revealed again that most of these combinations gave rise to measurable currents. In contrast to the duplication of CBS2 (upper panel), the duplication of CBS1 was compatible with channel function. However, a replacement by the CBS2 domain of IMPDH gave currents that were barely above background. Western blots such as those in Fig. 2C demonstrated that C<sub>721–988</sub> with CBS2 from ClC-5 or IMPDH stabilized N<sub>1–720</sub> to a similar extent as observed with C<sub>721–988</sub> (data not shown). Co-expression with epitope-tagged N<sub>1–720</sub> was used for some of these constructs to show that the decrease in current amplitude could be correlated with a decreased surface expression (Fig. 4D). Finally, a more detailed analysis of currents revealed that exchanging CBS domains often changed the voltage for half-maximal channel opening (Fig. 4E).

### Mutations in CBS domains affect gating

As our chimeric and deletion approach had suggested that CBS domains may influence gating, we mutated

---

dehydrogenase; 2↔1 indicates that CBS2 was replaced by CBS1 (lower panel), or that CBS1 was replaced by CBS2 (upper panel). The figure represents an independent experiment with  $n = 6$  oocytes. Another independent experiment gave similar results. *D*, surface expression of N<sub>1–720</sub> tagged with an extracellular HA epitope in the presence of different C<sub>721–988</sub> constructs in which the CBS2 domain of ClC-1 has been replaced by the indicated CBS2 domains, determined as in Fig. 1B. *E*, voltage values of half-activation for chimeras replacing CBS1 by CBS1 of the indicated proteins in ClC-1 and CBS2 by CBS2 of the indicated proteins in C<sub>721–988</sub>. Values were determined using a tail current analysis protocol, as described in Methods with two batches of oocytes, each batch containing  $n = 6$  oocytes.

single amino acids in CBS1 and CBS2 to study their potential effects on gating. To identify potentially interesting residues, we first created a model of a CBS1–CBS2 dimer of ClC-1, which was based on the crystal structure of CBS domains from bacterial IMPDH (Zhang *et al.* 1999). For modelling purposes, the two CBS domains of ClC-1 were connected by the region between CBS domains of IMPDH from *S. pyogenes* (Fig. 4B).

The two CBS domains interact with their  $\beta$ -strands to form a dimer (Fig. 4B). The two amphipathic  $\alpha$ -helices ( $\alpha_1$  and  $\alpha_2$ ) of each CBS domain contribute to the surface of this dimer. As protein–protein interactions occur through surface residues and often involve helix–helix interactions, amino acids at those sides of these helices that face the cytoplasm may potentially affect a putative CBS domain-dependent regulation, gating, or trafficking of ClC channels. Indeed, several osteopetrosis-causing mutations in ClC-7 (Kornak *et al.* 2001) changed residues located in  $\alpha$ -helices of CBS2 and that are predicted to face the cytoplasm (Estévez & Jentsch, 2002).

Based on the model (Figs 4B, and 5A and B), we selected residues that fulfilled the criteria described above. The chosen residues were always mutated to cysteine and to at least one amino acid that changed the electrical charge. After expression in *Xenopus* oocytes, their voltage dependence of gating was determined by tail current analysis.

None of the mutations in CBS1 changed the voltage of half-maximal activation ( $V_{0.5}$ ) significantly (Fig. 5A), whereas mutations of four CBS2 residues changed  $V_{0.5}$  by more than 10 mV (H835R, H838A, A862E/K and E865K; shown in red in Fig. 5B). The mutations H835R and H838A had the strongest effects. Depending on the mutation,  $V_{0.5}$  was shifted towards positive values (by  $\sim +60$  mV for H835R) or towards negative voltages (e.g. by  $\sim -20$  mV with H838A). The slope of  $P_{\text{open}}$  as a function of voltage was nearly unchanged and yielded a nominal gating charge of  $\sim 1$  as in WT ClC-1.

To investigate whether mutations in CBS domains affect the common gate or the gates that act on single protopores of the double-barrelled channel, the mutant having the strongest effect (H835R) was co-expressed with WT ClC-1 at a 1 : 1 ratio. The resulting voltage dependence of gating could not be explained by a linear superposition of WT and mutant currents, but suggested a dominant effect ( $V_{0.5}(\text{WT}) = -68.5 \pm 1.2$  mV ( $n = 68$ );  $V_{0.5}(\text{WT} + \text{H835R}) = -23.6 \pm 4$  mV ( $n = 6$ );  $V_{0.5}(\text{H835R}) = -11.8 \pm 2.4$  mV ( $n = 18$ )). This result strongly suggested that

this mutation affected the common gate (Saviane *et al.* 1999).

### Mutations in other ClC channels show a conserved role of CBS domains in modulating the common gate

The dominant effect of H853R on ClC-1 gating suggested an effect on the common gate (see above). In ClC-0, the common gate is very slow (in the range of seconds) and is opened by hyperpolarization, whereas the protopore gate is fast (in the millisecond range) and is activated by depolarization. These features greatly facilitate the distinction of both gates, also when using only macroscopic current measurements. Therefore, selected CBS2 point mutations were introduced into ClC-0 and studied in macropatches. The activation of the slow gate by preceding increasingly hyperpolarizing steps was tested during a constant ‘tail pulse’ after each sweep (Pusch *et al.* 1997; Fong *et al.* 1998) (Fig. 6A). In contrast to ClC-1, mutating ClC-0 Q733 (equivalent to H838 in ClC-1) to alanine or lysine did not significantly alter gating. However, mutating histidine 736 (equivalent to H838) to alanine completely eliminated the voltage dependence of the slow gate without significantly altering the fast gate that affects single pores (Fig. 6A). The mutation E763K (analogous to E865K in ClC-1) had similar effects (data not shown).

To explore further the hypothesis that mutations H736A and E763K locked the common gate of ClC-0 in the open state, we exploited the inhibitory effect of zinc ions. Extracellular zinc inhibits ClC-0 by binding preferentially to channels with a closed common gate (Chen, 1998). As a consequence, it was much less effective on the C212S mutant that locked this gate open (Lin *et al.* 1999). If the present mutants disabled the closure of the common gate, they should be less sensitive to zinc. Therefore, the effect of 10 and 100  $\mu\text{M}$   $\text{Zn}^{2+}$  was tested on currents from ClC-0 mutants H736A and E763K and compared to WT and C212S (Chen, 1998) mutant ClC-0 as negative and positive controls, respectively (Fig. 6B). Whereas 100  $\mu\text{M}$   $\text{Zn}^{2+}$  inhibited WT ClC-0 currents by  $\sim 60\%$ , the H736A mutant was as insensitive to  $\text{Zn}^{2+}$  as the C212S positive control ( $\sim 20\%$  inhibition), providing additional evidence that this CBS2 mutation abolishes slow gating. The E763K mutant showed an intermediate sensitivity.

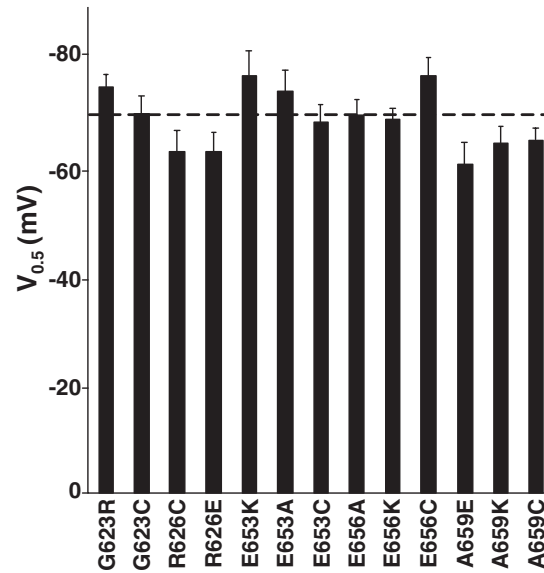
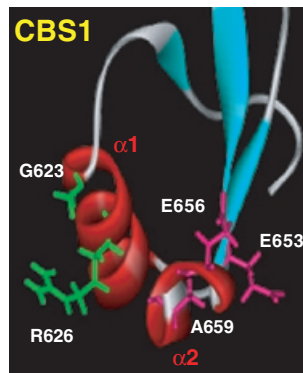
Mutants that affect the common gate may have dominant effects when co-expressed with WT channels. To investigate this issue, we constructed concatemers of ClC-0 which carried the mutations H736A or E763K only in the first or the second monomer, or in both monomers. As can

be seen in typical recordings in Fig. 6C, the presence of the mutation in only one of the monomers sufficed to abolish the slow gating of the dimer as revealed by the currents during the ‘tail pulse’. Similar results were obtained for the concatemers H736A~WT and H736A~H736A, as well as for concatemers containing the mutation E763K.

### Discussion

In contrast to those bacterial CLC proteins that have been crystallized (Dutzler *et al.* 2002), eukaryotic CLC channels have long cytoplasmic C-termini that range from 155 (CLC-Ks) to 398 amino acids (CLC-1) and that contain

A



B

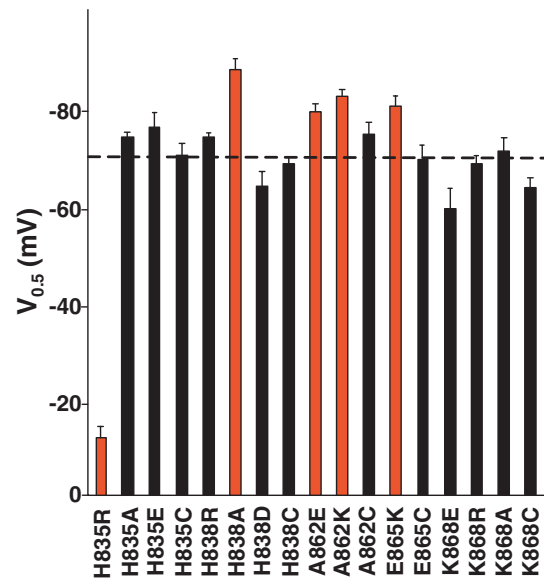
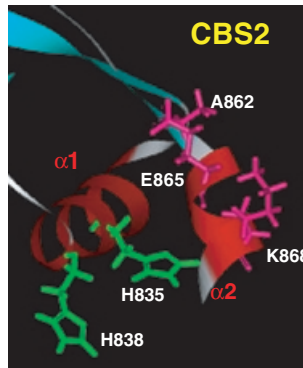


**Figure 5. Mutational analysis of charged amino acids from the  $\alpha$ -helices of CBS1 and CBS2 domains**

A, a detailed view of the helices from a homology model of the CBS1 domain of CIC-1, showing the amino acids that had been mutated and analysed functionally in oocytes. Amino acids from the first  $\alpha$ -helix are shown in green, and from the second  $\alpha$ -helix in pink. Right panel, values of the half-voltage of activation ( $V_{0.5}$ ) for mutants in the helices of the CBS1 domain of CIC-1 as determined by tail current analysis (see Methods). Experimental conditions were as in Fig. 4E. The dashed line corresponds to the value of the wild-type CIC-1. B, an analysis as in A of the CBS2 domain of CIC-1. Mutations that caused a deviation of  $V_{0.5}$  of more than 10 mV with respect to the wild-type value are marked in red.

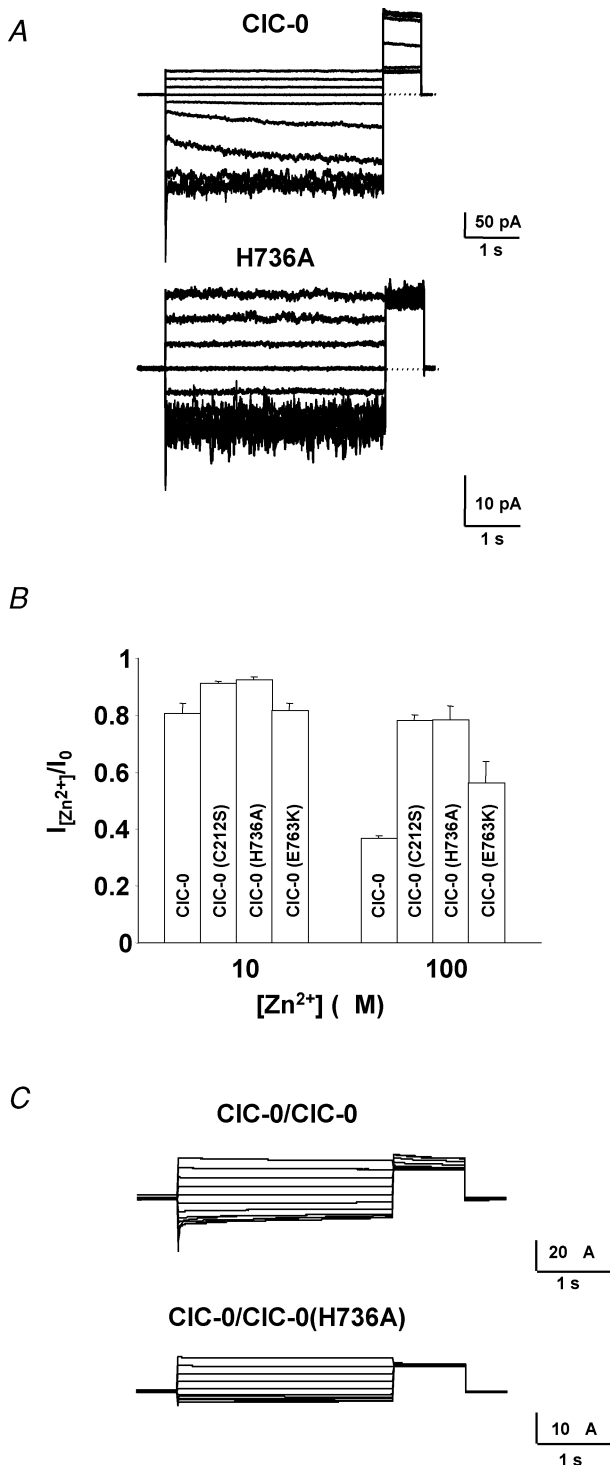


**Figure 6. Mutations in CIC-0 in the CBS2 domain influence the common gate**

A, typical patch clamp traces for CIC-0 and the CIC-0 mutation H736A (equivalent to H838A in CIC-1) filtered at 200 Hz. Inside-out macropatches were clamped between +60 and -120 mV in -20 mV steps for 4 s. The degree of activation of the slow gate at the end of the test pulse was monitored by the current during the constant 'tail' pulse to 60 mV. The traces shown in A are noisier than those in C and also than those in Fig. 3A because the patches contained a relatively

two so-called CBS domains. These structural domains, which contain a typical  $\beta 1-\alpha 1-\beta 2-\beta 3-\alpha 2$  fold, are present in many different proteins and in all phylae. Diverse functions have been postulated for these domains in different proteins (Estévez & Jentsch, 2002), but no clear role has emerged so far. The present work suggests that mutations in CBS domains affect protein-protein interactions *within* CLC protein subunits as well as *between* the two subunits of the dimer and that they influence the voltage dependence of gating through the common gate. Domain swapping revealed that CBS domains are largely interchangeable in their ability to support CLC channel function.

Experiments with 'split channels' suggested that the CBS domains (CBS1 and CBS2) that are present in the carboxy-terminus interact. As shown previously (Schmidt-Rose & Jentsch, 1997), CIC-1 gave no currents when it was truncated after CBS1 (N<sub>1-720</sub>). This was due to a failure to reach the plasma membrane (Fig. 1). Co-expression with the missing cytoplasmic part (C<sub>721-988</sub>) restored Cl<sup>-</sup> channel function, suggesting that the fragments bind each other, which was confirmed by coimmunoprecipitations. Deletions suggested that CBS2 and a short stretch immediately preceding it were crucial both for binding and for functional rescue, although CBS2 is dispensable when deleted in frame.

The amount of the N-terminal fragment N<sub>1-720</sub> was increased by co-expressing it with interaction-competent C-terminal fragments. This co-expression also increased the abundance of a monomeric form of N<sub>1-720</sub> at the expense of a putative SDS-resistant dimeric form. We suggest that CBS1 domains of two N<sub>1-720</sub> proteins may bind to each other in a dimeric, abnormal channel complex when they lack CBS2 as their normal binding partner. Such a homophilic CBS1-CBS1 binding is plausible as CBS1 could functionally replace CBS2 in the C-terminal fragment of the split channel (Fig. 4C). Whereas the abnormal N<sub>1-720</sub> dimer was quite stable in SDS, it could not reach the surface and was more rapidly degraded in

small number of channels compared to the two-electrode voltage clamp recordings of Figs 3A and 6C. The patch shown for the mutant contained fewer channels than that shown for WT explaining the noisier appearance of the mutant traces. B, analysis of zinc inhibition for CIC-0, CIC-0(C212S), CIC-0(H736A) and CIC-0(E763K) at 10 and 100  $\mu$ M. C, typical voltage clamp traces for the concatemer CIC-0/CIC-0(H736A) which affects the slow gate. A dominant effect on the activation of the slow gate as monitored during the constant tail pulse was observed. Similar results were obtained for the concatemers CIC-0(H736A)/CIC-0 and CIC-0(H736A)/CIC-0(H736A) and concatemers containing the E763K and C212S mutations.

the cell than WT dimers. Supplying CBS2 on a separate fragment would lead to preferential CBS1-CBS2 binding, thus yielding dimeric channels that can traffic to the surface and that may be metabolically more stable. These more 'normal' dimeric channels, however, are more easily dissociated by SDS than the N<sub>1-720</sub> proteins, resulting in the apparent increase of the monomeric form in Western blots. However, we could delete CBS2 in frame without abolishing channel function (Fig. 3), suggesting that the observed sorting defects and consequent loss of function (Fig. 2) resulted from an abnormal protein conformation rather than specific recognition of a lack of CBS1-CBS2 interactions.

The role of CBS domains in the correct targeting (possibly related to correct folding) of the channel is compatible with previous studies of the yeast CLC protein where mutations in CBS domains abolished its localization to the late Golgi that is seen upon overexpression (Schwappach *et al.* 1998). Mutations in the CBS2 domain in CLC-5 identified in patients with Dent's disease also resulted in missorting (Carr *et al.* 2003), and a mutation in CBS2 of CLC-7 led to undetectably low levels of the channel in fibroblasts from a patient with osteopetrosis (Kornak *et al.* 2001), pointing to a destabilization of the protein.

While the C-terminal fragment needed a CBS domain for binding to the N-terminal part and for functional rescue, the deletion of CBS2 within an otherwise intact CLC-1 protein led to functional channels. Thus, CLC channels do not strictly need two CBS domains in their C-terminus. In the split channel, the carboxy-terminal CBS domain may be needed to prevent misfolding of the cytoplasmic part of the protein, or may be required for the recruitment of other structures that are necessary for channel function. This may include the short stretch preceding CBS2, the deletion of which led to loss of function in both the otherwise intact channel and C<sub>721-988</sub>.

The fact that CBS domains from several CLC channels and even from the enzyme IMPDH could functionally substitute for CBS1 or CBS2 in CLC-1 indicates that the overall conservation of the 3-D structure, as opposed to the poorly conserved primary sequence, suffices for the interactions that are crucial for channel function (e.g. transport to the surface). On the other hand, we observed changes in voltage-dependent gating upon certain exchanges of CBS domains in CLC-1. Using site-directed mutagenesis, we identified several amino acids in  $\alpha$ -helices of CBS2 whose mutations led to changes in voltage dependence. The side chains of these amino acids are predicted to protrude from the surface of the CBS domain dimer, thus being

available for interactions with other parts of the channel or with other proteins that might bind to it. At this point, however, we ignore which of these possibilities – if any – is true.

The analysis of selected CBS mutants revealed that the common gate of CLC-1 and CLC-0 was affected. This conclusion was based on the dominant effect of the CLC-1 CBS2 mutant H835R on the gating of WT/mutant heteromers (Saviane *et al.* 1999), and, more directly, on the observation that the 'slow' (common) gating process of CLC-0 was abolished by two different CBS2 mutations (H736A and E763K). The latter mutation affects an anionic residue conserved in many CBS domains, with a mutation in the analogous CBS2 residue of IMPDH (D226N) being found in autosomal dominant retinitis pigmentosa (Bowne *et al.* 2002). The effects of CBS domain mutations on the common gate agree with previous experiments in which carboxy-terminal chimeras of CLC-0 with CLC-1 or CLC-2 changed the slow gate of CLC-0 (Fong *et al.* 1998). Obviously, CBS domains are not the only structures important for common gating, which must involve a coordinated conformational change of both channel subunits. Indeed, point mutations in the transmembrane block can also affect this gate (Pusch *et al.* 1995*b*; Lin *et al.* 1999; Saviane *et al.* 1999). Several residues that influence common gating reside at the interface between the CLC subunits (Estévez & Jentsch, 2002; Duffield *et al.* 2003). The structural basis of common gating is still unclear, but the very large temperature dependence of the slow gate of CLC-0 hinted at large conformational changes (Pusch *et al.* 1997). The present work suggests that the large C-termini of CLC channels, and in particular their CBS domains, participate in these changes. This would require an interaction of the transmembrane channel backbone with the cytoplasmic carboxy-terminus, which may involve non-covalent binding, or may be mediated by the polypeptide chain that links the CBS domains to the channel proper. The crystal structures of bacterial CLC proteins (Dutzler *et al.* 2002) offer intriguing insights in that respect: the last intramembrane helix, helix R, coordinates via its amino-terminal tyrosine a Cl<sup>-</sup> ion in the middle of the channel protein. This helix therefore directly links structures in the inner pore to the carboxy-terminus with its CBS domains and may thus have a role in gating. Furthermore, the amino-terminal helix A of one subunit is close to helix R in the crystal (Dutzler *et al.* 2002). This may suggest that both subunits also interact with their cytoplasmic structures; however, as the bacterial channels used for crystallization lack the large C-terminus and CBS domains, it is unclear whether this observation is relevant for the present results.

Most of the segment between CBS1 and CBS2, as well as the stretch following CBS2, could be deleted without abolishing channel function. However, these stretches may have important roles in interacting with other proteins. Indeed, a 'PY'-motif is found between CBS1 and CBS2 of CLC-5 that probably interacts with WW-domains of HECT-ubiquitin ligases (Schwake *et al.* 2001). Likewise, the region between the CBS domains of IMPDH was proposed to bind regulatory proteins (Zhang *et al.* 1999), and a splice variant of CLC-3 displays a PDZ-binding motif at its extreme carboxy-terminus (Ogura *et al.* 2002) that can interact with EBP50 (Ogura *et al.* 2002) and CAP70 (Gentzsch *et al.* 2003).

Interactions with other proteins might also occur via the CBS dimers. Although no binding partners for CLC CBS domains are known, it is intriguing that several CLC-7 mutations found in human osteopetrosis change CBS2 residues whose side chains are predicted to protrude from the surface of the CBS dimers (Estévez & Jentsch, 2002). Here we have shown that mutating several such 'surface residues' of CBS domains led to alterations in gating, maybe suggesting interactions with the channel backbone by non-covalent interactions. Determination of the structures of CBS-domain-containing C-termini of CLC channels, possibly by crystallization of bacterial CLC proteins that have CBS domains (Jentsch *et al.* 1999), and the identification of potential binding partners will be important future tasks.

CBS domains regulate the function of several other oligomeric proteins in which they occur. For instance, they have been implicated in the regulation of the enzyme CBS (Shan *et al.* 2001) and the  $\gamma 2$  subunit of AMP-activated protein kinase (Bowne *et al.* 2002). Although our work demonstrates that certain mutations in CBS domains affect CLC channel gating, physiologically relevant regulatory roles of CBS domains in CLC channels remain to be identified.

## References

- Bateman A (1997). The structure of a domain common to archaeobacteria and the homocystinuria disease protein. *Trends Biochem Sci* **22**, 12–13.
- Bauer CK, Steinmeyer K, Schwarz JR & Jentsch TJ (1991). Completely functional double-barreled chloride channel expressed from a single Torpedo cDNA. *Proc Natl Acad Sci USA* **88**, 11052–11056.
- Birkenhäger R, Otto E, Schürmann MJ, Vollmer M, Ruf EM, Maier-Lutz I *et al.* (2001). Mutation of *BSND* causes Bartter syndrome with sensorineural deafness and kidney failure. *Nat Genet* **29**, 310–314.
- Blair E, Redwood C, Ashrafian H, Oliveira M, Broxholme J, Kerr B *et al.* (2001). Mutations in the  $\gamma 2$  subunit of AMP-activated protein kinase cause familial hypertrophic cardiomyopathy: evidence for the central role of energy compromise in disease pathogenesis. *Hum Mol Genet* **10**, 1215–1220.
- Bowne SJ, Sullivan LS, Blanton SH, Cepko CL, Blackshaw S, Birch DG *et al.* (2002). Mutations in the inosine monophosphate dehydrogenase 1 gene (*IMPDH1*) cause the RP10 form of autosomal dominant retinitis pigmentosa. *Hum Mol Genet* **11**, 559–568.
- Carr G, Simmons N & Sayer J (2003). A role for CBS domain 2 in trafficking of chloride channel CLC-5. *Biochem Biophys Res Commun* **310**, 600–605.
- Chen TY (1998). Extracellular zinc ion inhibits CLC-0 chloride channels by facilitating slow gating. *J General Physiol* **112**, 715–726.
- Chen TY & Miller C (1996). Nonequilibrium gating and voltage dependence of the CLC-0 Cl<sup>-</sup> channel. *J General Physiol* **108**, 237–250.
- Cleiren E, Benichou O, Van Hul E, Gram J, Bollerslev J, Singer FR *et al.* (2001). Albers-Schönberg disease (autosomal dominant osteopetrosis, type II) results from mutations in the *CLCN7* chloride channel gene. *Hum Mol Genet* **10**, 2861–2867.
- Duffield M, Rychkov G, Bretag A & Roberts M (2003). Involvement of helices at the dimer interface in CLC-1 common gating. *J General Physiol* **121**, 149–161.
- Dutzler R, Campbell EB, Cadene M, Chait BT & MacKinnon R (2002). X-ray structure of a CLC chloride channel at 3.0 Å reveals the molecular basis of anion selectivity. *Nature* **415**, 287–294.
- Dutzler R, Campbell EB & MacKinnon R (2003). Gating the selectivity filter in CLC chloride channels. *Science* **300**, 108–112.
- Estévez R, Boettger T, Stein V, Birkenhäger R, Otto M, Hildebrandt F & Jentsch TJ (2001). Barttin is a Cl<sup>-</sup> channel  $\beta$ -subunit crucial for renal Cl<sup>-</sup> reabsorption and inner ear K<sup>+</sup>-secretion. *Nature* **414**, 558–561.
- Estévez R & Jentsch TJ (2002). CLC chloride channels: correlating structure and function. *Curr Opin Struct Biol* **12**, 531–539.
- Estévez R, Schroeder BC, Accardi A, Jentsch TJ & Pusch M (2003). Conservation of chloride channel structure revealed by an inhibitor binding site in CLC-1. *Neuron* **38**, 47–59.
- Fong P, Rehfeldt A & Jentsch TJ (1998). Determinants of slow gating in CLC-0, the voltage-gated chloride channel of *Torpedo marmorata*. *Am J Physiol* **274**, C966–C973.
- Gentzsch M, Cui L, Mengos A, Chang XB, Chen JH & Riordan JR (2003). The PDZ-binding chloride channel CLC-3B localizes to the Golgi and associates with CFTR-interacting PDZ proteins. *J Biol Chem* **278**, 6440–6449.

- Hryciw DH, Rychkov GY, Hughes BP & Bretag AH (1998). Relevance of the D13 region to the function of the skeletal muscle chloride channel, ClC-1. *J Biol Chem* **273**, 4304–4307.
- Jentsch TJ, Friedrich T, Schriever A & Yamada H (1999). The ClC chloride channel family. *Pflugers Arch* **437**, 783–795.
- Jhee KH, McPhie P & Miles EW (2000). Domain architecture of the heme-independent yeast cystathionine beta-synthase provides insights into mechanisms of catalysis and regulation. *Biochemistry* **39**, 10548–10556.
- Kennan A, Aherne A, Palfi A, Humphries M, McKee A, Stitt A et al. (2002). Identification of an IMPDH1 mutation in autosomal dominant retinitis pigmentosa (RP10) revealed following comparative microarray analysis of transcripts derived from retinas of wild-type and Rho (–/–) mice. *Hum Mol Genet* **11**, 547–557.
- Koch MC, Steinmeyer K, Lorenz C, Ricker K, Wolf F, Otto M et al. (1992). The skeletal muscle chloride channel in dominant and recessive human myotonia. *Science* **257**, 797–800.
- Kornak U, Kasper D, Bösl MR, Kaiser E, Schweizer M, Schulz A et al. (2001). Loss of the ClC-7 chloride channel leads to osteopetrosis in mice and man. *Cell* **104**, 205–215.
- Lin YW, Lin CW & Chen TY (1999). Elimination of the slow gating of ClC-0 chloride channel by a point mutation. *J General Physiol* **114**, 1–12.
- Lloyd SE, Pearce SH, Fisher SE, Steinmeyer K, Schwappach B, Scheinman S et al. (1996). A common molecular basis for three inherited kidney stone diseases. *Nature* **379**, 445–449.
- Ludewig U, Jentsch TJ & Pusch M (1997). Analysis of a protein region involved in permeation and gating of the voltage-gated *Torpedo* chloride channel ClC-0. *J Physiol* **498**, 691–702.
- Ludewig U, Pusch M & Jentsch TJ (1996). Two physically distinct pores in the dimeric ClC-0 chloride channel. *Nature* **383**, 340–343.
- Maduke M, Williams C & Miller C (1998). Formation of ClC-0 chloride channels from separated transmembrane and cytoplasmic domains. *Biochemistry* **37**, 1315–1321.
- Matsumura Y, Uchida S, Kondo Y, Miyazaki H, Ko SB, Hayama A et al. (1999). Overt nephrogenic diabetes insipidus in mice lacking the ClC-K1 chloride channel. *Nat Genet* **21**, 95–98.
- Middleton RE, Pheasant DJ & Miller C (1994). Purification, reconstitution, and subunit composition of a voltage-gated chloride channel from *Torpedo* electroplax. *Biochemistry* **33**, 13189–13198.
- Middleton RE, Pheasant DJ & Miller C (1996). Homodimeric architecture of a ClC-type chloride ion channel. *Nature* **383**, 337–340.
- Milan D, Jeon JT, Looft C, Amarger V, Robic A, Thelander M et al. (2000). A mutation in PRKAG3 associated with excess glycogen content in pig skeletal muscle. *Science* **288**, 1248–1251.
- Miller C & White MM (1984). Dimeric structure of single chloride channels from *Torpedo* electroplax. *Proc Natl Acad Sci U S A* **81**, 2772–2775.
- Ogura T, Furukawa T, Toyozaki T, Yamada K, Zheng YJ, Katayama Y et al. (2002). ClC-3B, a novel ClC-3 splicing variant that interacts with EBP50 and facilitates expression of CFTR-regulated ORCC. *Faseb J* **16**, S63–S65.
- Piwon N, Günther W, Schwake R, Bösl MR & Jentsch TJ (2000). ClC-5 Cl<sup>–</sup> channel disruption impairs endocytosis in a mouse model for Dent's disease. *Nature* **408**, 369–373.
- Ponting CP (1997). CBS domains in ClC chloride channels implicated in myotonia and nephrolithiasis (kidney stones). *J Mol Med* **75**, 160–163.
- Pusch M, Accardi A, Liantonio A, Ferrera L, De Luca A, Camerino DC & Conti F (2001). Mechanism of block of single protopores of the *Torpedo* chloride channel ClC-0 by 2-(p-chlorophenoxy) butyric acid (CPB). *J General Physiol* **118**, 45–62.
- Pusch M, Jordt SE, Stein V & Jentsch TJ (1999). Chloride dependence of hyperpolarization-activated chloride channel gates. *J Physiol* **515**, 341–353.
- Pusch M, Ludewig U & Jentsch TJ (1997). Temperature dependence of fast and slow gating relaxations of ClC-0 chloride channels. *J General Physiol* **109**, 105–116.
- Pusch M, Ludewig U, Rehfeldt A & Jentsch TJ (1995a). Gating of the voltage-dependent chloride channel ClC-0 by the permeant anion. *Nature* **373**, 527–531.
- Pusch M, Steinmeyer K, Koch MC & Jentsch TJ (1995b). Mutations in dominant human myotonia congenita drastically alter the voltage dependence of the ClC-1 chloride channel. *Neuron* **15**, 1455–1463.
- Richard EA & Miller C (1990). Steady-state coupling of ion-channel conformations to a transmembrane ion gradient. *Science* **247**, 1208–1210.
- Sali A & Blundell TL (1993). Comparative protein modelling by satisfaction of spatial restraints. *J Mol Biol* **234**, 779–815.
- Saviane C, Conti F & Pusch M (1999). The muscle chloride channel ClC-1 has a double-barreled appearance that is differentially affected in dominant and recessive myotonia. *J General Physiol* **113**, 457–468.
- Schmidt-Rose T & Jentsch TJ (1997). Reconstitution of functional voltage-gated chloride channels from complementary fragments of ClC-1. *J Biol Chem* **272**, 20515–20521.
- Schwake M, Friedrich T & Jentsch TJ (2001). An internalization signal in ClC-5, an endosomal Cl<sup>–</sup> channel mutated in Dent's disease. *J Biol Chem* **276**, 12049–12054.
- Schwake M, Pusch M, Kharkovets T & Jentsch TJ (2000). Surface expression and single channel properties of KCNQ2/KCNQ3, M-type K<sup>+</sup> channels involved in epilepsy. *J Biol Chem* **275**, 13343–13348.

- Schwappach B, Stobrawa S, Hechenberger M, Steinmeyer K & Jentsch TJ (1998). Golgi localization and functionally important domains in the NH<sub>2</sub> and COOH terminus of the yeast CLC putative chloride channel Gef1p. *J Biol Chem* **273**, 15110–15118.
- Shan X, Dunbrack RL, Christopher SA & Kruger WD (2001). Mutations in the regulatory domain of cystathionine beta synthase can functionally suppress patient-derived mutations in cis. *Hum Mol Genet* **10**, 635–643.
- Shan X & Kruger WD (1998). Correction of disease-causing CBS mutations in yeast. *Nat Genet* **19**, 91–93.
- Simon DB, Bindra RS, Mansfield TA, Nelson-Williams C, Mendonca E, Stone R et al. (1997). Mutations in the chloride channel gene, CLCNKB, cause Bartter's syndrome type III. *Nat Genet* **17**, 171–178.
- Sintchak MD, Fleming MA, Futer O, Raybuck SA, Chambers SP, Caron PR et al. (1996). Structure and mechanism of inosine monophosphate dehydrogenase in complex with the immunosuppressant mycophenolic acid. *Cell* **85**, 921–930.
- Sippl MJ (1993). Recognition of errors in three-dimensional structures of proteins. *Proteins* **17**, 355–362.
- Steinmeyer K, Klocke R, Ortland C, Gronemeier M, Jockusch H, Gründer S & Jentsch TJ (1991). Inactivation of muscle chloride channel by transposon insertion in myotonic mice. *Nature* **354**, 304–308.
- Stobrawa SM, Breiderhoff T, Takamori S, Engel D, Schweizer M, Zdebik AA et al. (2001). Disruption of CLC-3, a chloride channel expressed on synaptic vesicles, leads to a loss of the hippocampus. *Neuron* **29**, 185–196.
- Weinreich F & Jentsch TJ (2001). Pores formed by single subunits in mixed dimers of different CLC chloride channels. *J Biol Chem* **276**, 2347–2353.
- Zerangue N, Schwappach B, Jan YN & Jan LY (1999). A new ER trafficking signal regulates the subunit stoichiometry of plasma membrane K<sub>ATP</sub> channels. *Neuron* **22**, 537–548.
- Zhang R, Evans G, Rotella FJ, Westbrook EM, Beno D, Huberman E et al. (1999). Characteristics and crystal structure of bacterial inosine-5'-monophosphate dehydrogenase. *Biochemistry* **38**, 4691–4700.

### Acknowledgements

We thank J. Enderich for technical assistance. R.E. is a recipient of a Marie Curie Human Potential Fellowship of the European Union. This work was supported by grants from the DFG, the Fonds der Chemischen Industrie, and the Prix Louis Jeantet de Médecine to T.J.J., and from Telethon Italy (grant 1079) and the Italian Research Ministry (FIRB RBAU01PJMS) to M.P.

### Author's Present Address

R. Estévez: Institute de Recerca Biomédica, Parc Científic de Barcelona, C/Josep Samitier 1–5, Barcelona 08028, Spain.